chemistry proceedings

MDPI

Proceeding Paper

Evaluation Electronic Properties of Rufinamide via Ab-Initio Study as Anti-Epileptic Drug †

Vaibhav Pandey, Mohd. Faheem, Sachin Ranjan and Manish Dixit *

Department of Nuclear Medicine, Sanjay Gandhi Postgraduate Institute of Medical Sciences, Lucknow 226014, UP, India; vaibhavparasar94@gmail.com (V.P.); faheemurfi@gmail.com (M.F.); androidlucky@gmail.com (S.R.)

* Correspondence: dixitm@sgpgi.ac.in

† Presented at the 28th International Electronic Conference on Synthetic Organic Chemistry (ECSOC-28), 15–30 November 2024; Available online: https://sciforum.net/event/ecsoc-28.

Abstract: The FDA approved rufinamide, chemically 1-(2,6-difluorobenzyl)-1H-1,2,3-triazole-4-carboxamide, a triazole-based scaffold, as an anticonvulsant drug in 2008. It is mainly used to treat seizures associated with Lennox–Gastaut Syndrome (LGS). The exact mechanism of rufinamide is unknown, but some literature reported that rufinamide works by regulating the brain's sodium channel activity, which aids in maintaining the stability of neuronal membranes and averting the overabundance of electrical activity. In the view of computational chemistry, the amide group, fluorine atom, and triazole ring are the specific parts of this skeleton and play an important role in action with the receptor. This study explored computerized simulations of quantum chemistry techniques to investigate the chemical structure and electrical properties of rufinamide. An optimizing structure started the quantum calculation through the B3LYP 6311-G (++, d, p) basis set, explored along with investigating the maximal quantity of electronic charge transfer (N_{max}), chemical hardness (η), electrostatic potential, chemical potential (μ), and electrophilicity (ω). The Natural Bond Orbital (NBO) analysis-based observation reveals that the molecule's chemically active regions have hyperconjugated electron interactions within the molecule, which contributes to the molecule's stability. This study explores the role of the amide group and difluoro-substituted phenyl group in chemical structure and in binding property with the receptor of the Ca^{2+}–and voltage-activated K^+ channel.

Keywords: rufinamide; DFT; neurotransmitters; seizures; epilepsy

check for updates

Citation: Pandey, V.; Faheem, M.; Ranjan, S.; Dixit, M. Evaluation Electronic Properties of Rufinamide via Ab-Initio Study as Anti-Epileptic Drug. *Chem. Proc.* **2024**, *16*, 16. https://doi.org/10.3390/ecsoc-28-20205

Academic Editor: Julio A. Seijas

Published: 14 November 2024

Copyright: © 2024 by the authors. Licensee MDPI, Basel, Switzerland. This article is an open access article distributed under the terms and conditions of the Creative Commons Attribution (CC BY) license (https://creativecommons.org/licenses/by/4.0/).

1. Introduction

Rufinamide (RFM, 1-((2,6-difluorophenyl)methyl)-1*H*-1,2,3-triazole-4-carboxamide) is a triazole derivative with an amide group known to have antiepileptic properties [1]. It is being used more frequently in combination with other drugs and treatments to treat various seizure disorders, Lennox–Gastaut syndrome, and severe epileptic encephalopathy [2,3]. RFM has a favorable cognitive side-effect profile and has been demonstrated to reduce the frequency and intensity of seizures linked to Lennox–Gastaut syndrome [4]. However, the answer to whether and how RFM affects transmembrane ionic currents in a coordinated manner is unknown [4,5].

The electronic structure of molecules is studied using Density Functional Theory (DFT), a quantum mechanical modelling technique that is especially useful for comprehending the physical characteristics of RFM. The DFT provides insights into the molecular geometry, electronic distribution and potential energy surfaces of RFM, aiding in the prediction of its chemical reactivity and interaction with biological targets. Using DFT, researchers can calculate the optimized structure of RFM, allowing for a detailed analysis of bond lengths, angles, and conformational stability. The stability and reactivity of the compound can be

ascertained by determining its electronic characteristics, such as its lowest unoccupied molecular orbital (LUMO) and highest occupied molecular orbital (HOMO) energies. DFT also aids in comprehending the molecule's electron density distribution, which is crucial for predicting how RFM interacts with its biological targets, such as sodium channels or potassium/calcium channels involved in seizure activity. This chemical skeleton's triazole, fluorine, and amide groups are crucial in their interactions with the residues of the active site. RFM is thought to bind to the intracellular domain of potassium/calcium channels, according to molecular docking. The amino acids Asn427, Asn808, and Ile810 establish hydrogen bonds with the electronegative binding sites of RFM, according to Huang et al., 2022. Furthermore, hydrophobic interactions are noted with Tyr429, Asn809, and His350 amino acids [5]. In this article, we apply the DFT to enhance the understanding of RFM behavior with the receptor by the physical properties.

2. Materials and Methods

The molecule was first designed in ChemDraw 16.0 software and saved in .cdx file format. Chem3D 16.0 software was used to create three-dimensional models of every chemical system that was analyzed.

Subsequently, the structure was pre-optimized by the universal force field (UFF) in the Avogadro program [6]. The RFM quantum chemical computations were performed at the DFT/B3LYP level of theory with the Gaussian 09W program suite [7–11] and the 6311-G (++, d, p) set. The UV spectra of the molecule electrostatic potential surfaces and optimized geometrical parameters were all determined using the Gaussview 6.0 program [10,11]. By applying the finite field method (FF) at a single location on the previously optimized geometries, the electric dipole moments (μ), first-order hyperpolarizability (β), and polarizability (α) values were determined [12–14].

3. Results and Discussion

3.1. Structural Parameter Optimization

To explain computational biological properties, a crucial step in molecular modeling is selecting a level of theory that is both computationally feasible and yields accurate equilibrium geometries compared to experimentally obtained molecular geometries for a potent scaffold targeting a specific molecule. In this study, DFT was chosen along with the 6-311G(d,p) basis set to perform molecular optimization calculations. This combination of method and basis set effectively described the geometric parameters of the RFM molecule (Figure 1). Table 1 presents the theoretically calculated bond lengths, bond angles, and dihedral angle values of the RFM structure using the 6-311G(++,d,p) basis set. The RFM structure belongs to the C1 point group symmetry. Figure 1 illustrates the optimized molecular structure, and Table 1 provides the theoretical data.

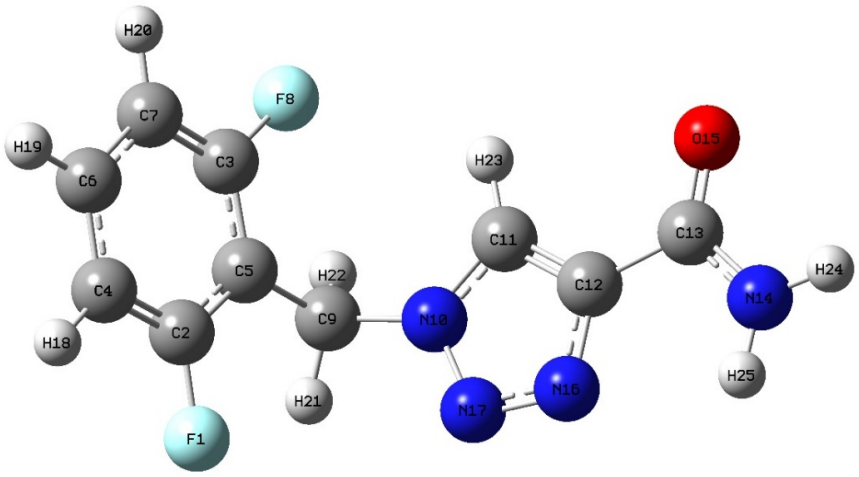


Figure 1. Optimized structure of RFM skeleton.

Table 1. Bond parameters of the optimized RFM skeleton.

Bond Length (A°)		Bond Angle (°)		Dihedral Angle (°)	
C4C2	1.385	C5C2C4	123.194	C3C5C2C4	0.196
C5C2	1.394	C3C5C2	115.806	C6C4C2C5	−0.17
C3C5	1.394	C6C4C2	118.476	C7C3C5C2	−0.127
C6C4	1.393	C7C3C5	123.525	F1C2C4C5	118.014
C7C3	1.384	F1C2C4	118.79	F8C3C5C7	118.919
F1C2	1.353	F8C3C5	117.557	C9C5C2C3	121.949
F8C3	1.356	C9C5C2	122.242	N10C9C5C2	−94.454
C9C5	1.508	N10C9C5	113.002	C11N10C9C5	−77.413
N10C9	1.47	C11N10C9	129.105	N17N10C9C11	110.863
C11N10	1.349	N17N10C9	120.013	C12C11N10C9	178.629
N17N10	1.353	C12C11N10	104.217	N16N17N10C9	−178.809
C12C11	1.378	N16N17N10	107.421	C13C12C11N16	123.87
N16N17	1.299	C13C12C11	127.833	H20C7C3C6	122.003
C13C12	1.484	H20C7C3	119.783	N14C13C12C11	−179.554
H20C7	1.082	N14C13C12	114.477	O15C13C12N14	124.244
N14C13	1.351	O15C13C12	121.279	H18C4C2C6	121.894
O15C13	1.228	H18C4C2	119.63	H19C6C4C7	119.596
H18C4	1.082	H19C6C4	119.619	H23C11N10C12	132.476
H19C6	1.083	H23C11N10	123.307	H21C9C5N10	105.857
H23C11	1.076	H21C9C5	110.544	H22C9C5N10	107.796
H21C9	1.087	H22C9C5	110.69	H24N14C13C12	−179.768
H22C9	1.089	H24N14C13	119.595	H25N14C13H24	119.696
H24N14	1.008	H25N14C13	120.709		
H25N14	1.008				

3.2. Electronic Properties

The Highest Occupied Molecular Orbital (HOMO) and Lowest Unoccupied Molecular Orbital (LUMO) are the two molecular orbital boundaries that play a key role in chemical reactivity. In chemical reactions, the HOMO acts as an electron donor, whereas the LUMO acts as an acceptor by its surface. The energy difference between the HOMO and LUMO, referred to as the frontier energy gap (ΔE_{gap}), characterizes a molecular system's hardness or softness, kinetic stability, optical polarizability, and chemical reactivity. Generally, the systems with a low HOMO-LUMO gap (ΔE_{gap}) are associated with low kinetic stability and high chemical reactivity, indicating a soft electronic system. For UV-Vis electronic spectrum studies, RFM was dissolved in methanol. The TD-DFT method was applied to the theoretical analysis of the electronic spectrum with a basis set of B3LYP/6-311++g(d,p). The primary RFM contributions are shown in Table 2, together with the oscillator strengths (f), excitation energies (E), and wavelengths (λ). Three bands were found in the theoretical electronic spectra at 239.10 nm, 220.86 nm, and 243.93 nm. To evaluate the RFM chemical stability, the HOMO and LUMO energy gaps were calculated to assess the RFM chemical stability. The HOMO, HOMO-1, HOMO-2, and LUMO orbitals are shown in Figure 2, together with the corresponding energies and energy gaps. Table 2 indicates that the HOMO-LUMO energy gap is ~6.04 eV and shows higher chemical stability. In HOMO-LUMO pictorial representations, the positive phases are yellow and the negative phases are green in color.

Table 2. The excitation energy E (eV) and theoretical absorption wavelength λ (nm) of RFM using the 6-311++g(d,p) basis set and B3LYP functional.

SN	Electronic Transitions (Molecular Orbitals Involved)	Energy (in eV)	Oscillatory Strength (f)	Calculated λmax in nm (B3LYP)
01	HOMO→LUMO	6.04	0.0191	239.10
02	HOMO-1→LUMO	6.31	0.0004	220.86
03	HOMO-2→LUMO	6.45	---	243.93
04	Urea	7.36	---	---

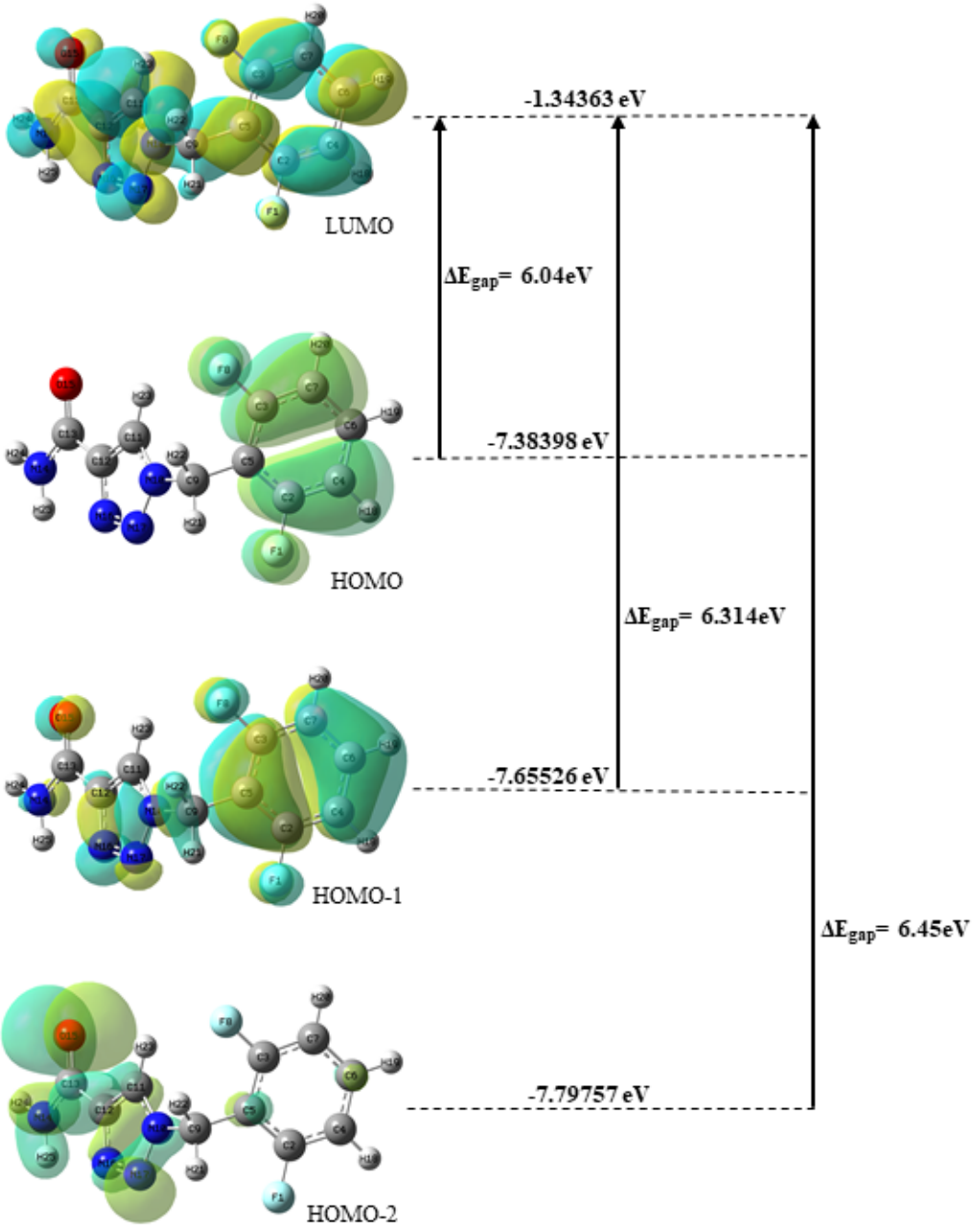


Figure 2. Molecular orbitals (HOMO→LUMO, HOMO-1→LUMO, and HOMO-2→LUMO) of RFM at the B3LYP/6-311++g(d,p) basis set.

3.3. Molecular Electrostatic Potential Surface (MEPs)

A molecular electrostatic potential surface is applied for the calculation of nucleophilicity and electrophilicity of RFM computationally. These surfaces indicate electronic density variation with a change in color. The molecular surface of RFM is represented by a color scale ranging from red to blue: -6.830×10^{-2} to 6.830×10^{-2} a.u. The red regions depict areas of highest electron repulsion and the blue areas signify regions of strongest electron attraction as depicted in Figure 3. The pictorial representation shows that the benzyl group has electron-deficient zones as shown in blue and that the oxygen atom in the amide group has electron-rich regions as shown in red in Figure 3.

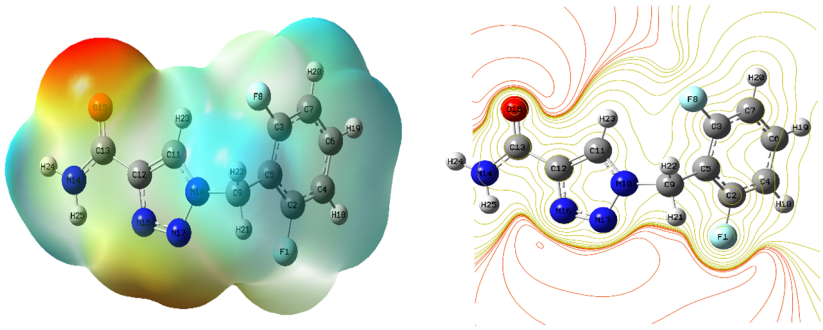


Figure 3. Molecular electrostatic surface potential surface (MEPs) analysis of RFM.

3.4. Global Reactivity Descriptors

The terms used to explain global reactivity are electronegativity (χ), global hardness (η), chemical potential (μ), electrophilicity index (ω), etc. These are utilized in the computation of the molecular systems' chemical reactivity and site selectivity by DCT calculation. The global reactivity descriptors values can be calculated by using Koopman's theorem with HOMO and LUMO energies [15–19].

$$Ionization\ potential\ (IP) = -\varepsilon_{HOMO} \quad (1)$$

$$Electron\ affinity\ (EA) = -\varepsilon_{LUMO} \quad (2)$$

$$Electronegativity\ (\chi) = -\frac{1}{2}(\varepsilon_{LUMO} + \varepsilon_{HOMO}) \quad (3)$$

$$Global\ hardness\ (\eta) = \frac{1}{2}(\varepsilon_{LUMO} - \varepsilon_{HOMO}) \quad (4)$$

$$Chemical\ potential\ (\mu) = -\chi = \frac{1}{2}(\varepsilon_{LUMO} + \varepsilon_{HOMO}) \quad (5)$$

$$Electrophilicity\ index\ (\omega) = \frac{\mu^2}{2\eta} \quad (6)$$

$$(\triangle N_{\max}) = \frac{-\mu}{\eta} \quad (7)$$

The hardness of the molecule is related to stability and it is calculated by the energy gap between the HOMO and LUMO. From the theoretical calculations, the HOMO and LUMO energy gap and global reactivity parameters of the RFM molecule are summarized in Table 3.

Table 3. Global reactive descriptor values.

Compound	ε_H	ε_L	ε_L-ε_H	IP	EA	χ	η	μ	ω	δN_{max}
RFM	−7.38	−1.34	6.04	7.38	1.34	4.18	3.02	−4.18	3.49	1.38

3.5. Nonlinear Optical Properties

The large first-order hyperpolarizabilities of molecules are key to nonlinear optical properties. These properties have wide-ranging applications in engineering, physics, and chemistry. When subjected to an electric field, a molecule's hyperpolarizability, polarizability, and dipole moment exhibit unique characteristics. The average linear polarizability (αtot), mean first-order hyperpolarizability (βtot), and total static dipole moment (μtot) can be determined using the x, y, and z components.

$$dipole\ moment\ (\mu_{tot}) = (\mu^2{}_x + \mu^2{}_y + \mu^2{}_z)^{1/2} \quad (8)$$

$$polarizibality\ (\alpha_{tot}) = \frac{1}{3}(\alpha_{xx} + \alpha_{yy} + \alpha_{zz}) \quad (9)$$

$$hyperpolarizability\ (\beta_{tot}) = [(\beta_{xxx} + \beta_{xyy} + \beta_{xzz})^2 + (\beta_{yyy} + \beta_{yxx} + \beta_{yzz})^2 + (\beta_{zzz} + \beta_{zxx} + \beta_{zyy})^2]^{1/2} \quad (10)$$

To evaluate the NLO properties of RFM, the total molecular polarizability (α_{tot}), along with its components, the total molecular dipole moment (μ_{tot}) and the first-order hyperpolarizability (β_{tot}) were calculated. The results are presented in Table 4. The electronic dipole moment (μ_{tot}) was found to be 2.669 Debye, while the first-order hyperpolarizability of RFM was measured at 173.848 esu. The significant hyperpolarizability value suggests that the NLO behavior of the system is associated with intramolecular charge transfer.

Table 4. Dipole moment (μ_{total}), polarizability (α_{total}), and hyperpolarizability (β_{total}) of RFM.

Dipole Moment		**Polarizability**		**Hyperpolarizability**	
μ_x	1.6759991	α_{xx}	179.5048736	β_{xxx}	3.4307371
μ_y	0.0290843	α_{yy}	5.1002585	β_{yyy}	120.5448139
μ_z	−2.0780206	α_{zz}	150.8724504	β_{zzz}	78.9210451
μ_{tot} (D)	2.669	α_{xy}	−6.1887669	β_{xyy}	13.6938889
		α_{xz}	0.8133262	β_{xxy}	−27.5238732
		α_{yz}	108.409047	β_{xxz}	78.6629049
		α_0 (esu)	111.828	β_{xzz}	−19.8625254
				β_{yzz}	−6.0133395
				β_{yyz}	−7.1003707
				β_{xyz}	−65.2994778
				β_0 (esu)	173.848

4. Conclusions

This study investigates the structural and electronic characteristics of RFM using quantum chemistry simulations through DFT calculations. The HOMO-LUMO plots were utilized to assess the chemical stability of RFM, focusing on the energy gap between HOMO and LUMO, which indicates the reactive sites of the molecule. The MESP surfaces were analyzed to identify electronic-poor and electronic-rich regions. The computed small energy gap between HOMO and LUMO confirmed charge transfer, suggesting lower kinetic stability and higher chemical reactivity, facilitating NLO activity. Additionally, the calculated first-order hyperpolarizability and dipole moment values further supported the NLO-active nature of the RFM. The molecular analysis of RFM via DFT provides substantial information about its structural and electronic characteristics, which correlate with its anticonvulsant properties. The study's insights pave the way for future research on RFM derivatives and their applications in neurotherapeutics and diagnostics.

Author Contributions: V.P. and M.F.: investigation, methodology, data correction, original draft, editing, communication, S.R.: data correction, editing, M.D.: supervision, review and editing. All authors have read and agreed to the published version of the manuscript.

Funding: We sincerely acknowledge the financial support provided by ICMR-DHR New Delhi for this research. The fellowship granted to Vaibhav Pandey through Grant Number: 11013/24/2021-GIA/HR has been instrumental in facilitating this study.

Institutional Review Board Statement: Not applicable.

Informed Consent Statement: Not applicable.

Data Availability Statement: Data are contained within the article.

Conflicts of Interest: The authors declare no conflict of interest.

References

1. Das, N.; Dhanawat, M.; Shrivastava, S.K. An Overview on Antiepileptic Drugs. *Drug Discov. Ther.* **2012**, *6*, 178–193. [CrossRef]
2. Rijckevorsel, K. Treatment of Lennox-Gastaut Syndrome: Overview and Recent Findings. *Neuropsychiatr. Dis. Treat.* **2008**, *1001*, 1001–1019. [CrossRef] [PubMed]
3. Cross, J.H.; Auvin, S.; Falip, M.; Striano, P.; Arzimanoglou, A. Expert Opinion on the Management of Lennox–Gastaut Syndrome: Treatment Algorithms and Practical Considerations. *Front. Neurol.* **2017**, *8*, 505. [CrossRef] [PubMed]
4. Sankar, R.; Chez, M.; Pina-Garza, J.E.; Dixon-Salazar, T.; Flamini, J.R.; Hyslop, A.; McGoldrick, P.; Millichap, J.J.; Resnick, T.; Rho, J.M.; et al. Proposed Anti-Seizure Medication Combinations with Rufinamide in the Treatment of Lennox-Gastaut Syndrome: Narrative Review and Expert Opinion. *Seizure Eur. J. Epilepsy* **2023**, *110*, 42–57. [CrossRef] [PubMed]
5. Lai, M.-C.; Wu, S.-N.; Huang, C.-W. Rufinamide, a Triazole-Derived Antiepileptic Drug, Stimulates Ca2+-Activated K+ Currents While Inhibiting Voltage-Gated Na+ Currents. *Int. J. Mol. Sci.* **2022**, *23*, 13677. [CrossRef] [PubMed]
6. Hanwell, M.D.; Curtis, D.E.; Lonie, D.C.; Vandermeersch, T.; Zurek, E.; Hutchison, G.R. Avogadro: An Advanced Semantic Chemical Editor, Visualization, and Analysis Platform. *J. Cheminform.* **2012**, *4*, 17. [CrossRef] [PubMed]
7. Kohn, W.; Sham, L.J. Self-Consistent Equations Including Exchange and Correlation Effects. *Phys. Rev.* **1965**, *140*, A1133–A1138. [CrossRef]
8. Becke, A.D. Density-Functional Thermochemistry. I. The Effect of the Exchange-Only Gradient Correction. *J. Chem. Phys.* **1992**, *96*, 2155–2160. [CrossRef]
9. Lee, C.; Yang, W.; Parr, R.G. Development of the Colle-Salvetti Correlation-Energy Formula into a Functional of the Electron Density. *Phys. Rev. B* **1988**, *37*, 785–789. [CrossRef]
10. Frisch, M.J.; Trucks, G.W.; Schlegel, H.B.; Scuseria, G.E.; Robb, M.A.; Cheeseman, J.R.; Scalmani, G.; Barone, V.; Mennucci, B.; Petersson, G.A.; et al. *Gaussian 09*; Gaussian: Wallingford, CT, USA, 2009; pp. 150–166.
11. Becke, A.D. Density functional thermochemistry. III The role of exact exchange. *J. Chem. Phys.* **1993**, *93*, 5648. [CrossRef]
12. Kleinman, D.A. Nonlinear Dielectric Polarization in Optical Media. *Phys. Rev.* **1962**, *126*, 1977–1979. [CrossRef]
13. Pipek, J.; Mezey, P.G. A Fast Intrinsic Localization Procedure Applicable for ab initio and Semiempirical Linear Combination of Atomic Orbital Wave Functions. *J. Chem. Phys.* **1989**, *90*, 4916–4926. [CrossRef]
14. Krishnakumar, V.; Keresztury, G.; Sundius, T.; Ramasamy, R. Simulation of IR and Raman Spectra Based on Scaled DFT Force Fields: A Case Study of 2-(Methylthio)Benzonitrile, with Emphasis on Band Assignment. *J. Mol. Struct.* **2004**, *702*, 9–21. [CrossRef]
15. Gritsenko, O.V. Koopmans' Theorem and Its Density-Functional-Theory Analog Assessed in Evaluation of the Red Shift of Vertical Ionization Potential upon Complexation. *Chem. Phys. Lett.* **2018**, *691*, 178–180. [CrossRef]
16. Pearson, R.G. Absolute Electronegativity and Hardness: Applications to Organic Chemistry. *J. Org. Chem.* **1989**, *54*, 1423–1430. [CrossRef]
17. Parr, R.G.; Szentpály, L.v.; Liu, S. Electrophilicity Index. *J. Am. Chem. Soc.* **1999**, *121*, 1922–1924. [CrossRef]
18. Chattaraj, P.K.; Giri, S. Stability, Reactivity, and Aromaticity of Compounds of a Multivalent Superatom. *J. Phys. Chem. A* **2007**, *111*, 11116–11121. [CrossRef] [PubMed]
19. Padmanabhan, J.; Parthasarathi, R.; Subramanian, V.; Chattaraj, P.K. Electrophilicity-Based Charge Transfer Descriptor. *J. Phys. Chem. A* **2007**, *111*, 1358–1361. [CrossRef] [PubMed]

Disclaimer/Publisher's Note: The statements, opinions and data contained in all publications are solely those of the individual author(s) and contributor(s) and not of MDPI and/or the editor(s). MDPI and/or the editor(s) disclaim responsibility for any injury to people or property resulting from any ideas, methods, instructions or products referred to in the content.